

CERN-TH/97-310
DTP/97/98
UCL/HEP 97-08
November 1997

Photoproduction Processes in Polarized ep - Collisions at HERA

J.M. Butterworth^a, N. Goodman^a, M. Stratmann^b, W. Vogelsang^c

^a*Department of Physics and Astronomy, University College London,
Gower Street, London WC1E 6BT, England*

^b*Department of Physics, University of Durham, Durham DH1 3LE, England*

^c*Theoretical Physics Division, CERN, CH-1211 Geneva 23, Switzerland*

Abstract

We study various conceivable photoproduction reactions in a polarized ep collider mode of HERA with respect to their sensitivity to the proton's polarized gluon distribution. A special emphasis is put on the 'resolved' part of the cross sections which in principle opens the possibility to determine for the first time also the completely unknown parton content of longitudinally polarized photons. In the very promising case of dijet production we also investigate the impact of parton showering, hadronization and jet finding on the parton level results.

Photoproduction Processes in Polarized ep - Collisions at HERA

J.M. Butterworth^a, N. Goodman^a, M. Stratmann^b, W. Vogelsang^c

^a*Department of Physics and Astronomy, University College London,
Gower Street, London WC1E 6BT, England*

^b*Department of Physics, University of Durham, Durham DH1 3LE, England*

^c*Theoretical Physics Division, CERN, CH-1211 Geneva 23, Switzerland*

Abstract

We study various conceivable photoproduction reactions in a polarized ep collider mode of HERA with respect to their sensitivity to the proton's polarized gluon distribution. A special emphasis is put on the 'resolved' part of the cross sections which in principle opens the possibility to determine for the first time also the completely unknown parton content of longitudinally polarized photons. In the very promising case of dijet production we also investigate the impact of parton showering, hadronization and jet finding on the parton level results.

1 Introduction

Despite the recent experimental progress in the field of polarized deep-inelastic scattering (DIS), the presently available data sets of inclusive and semi-inclusive DIS are still not sufficient to accurately fix the spin-dependent parton distributions $\Delta f(x, Q^2)$ of the nucleons, in particular they hardly constrain the gluon density Δg [1-3]. Even less satisfactory is the situation for the $\Delta f^\gamma(x, Q^2)$, the parton distributions of longitudinally (more precisely, circularly) polarized photons, where nothing at all is known experimentally.

In past years, HERA has already been very successful in pinning down the proton's unpolarized gluon distribution $g(x, Q^2)$ from observations of scaling violations in increasingly accurate $F_2(x, Q^2)$ measurements and from several exclusive processes such as jet, large- p_T hadron, and heavy flavour production. Moreover, since the bulk of the HERA events originates from the photoproduction region ($Q^2 \rightarrow 0$), 'resolved' processes have been measured, in which the (quasi-real) photon interacts not only in a 'direct' ('point-like') way but resolves into its hadronic structure. These HERA measurements [4-13] have been precise enough to improve not only our knowledge about the parton content of the unpolarized proton, but even about that of the photon, f^γ .

Given the success of such unpolarized photoproduction experiments at HERA, it seems to be quite natural to closely examine the same processes also for the situation with longitudinally polarized beams, in order to determine their sensitivity to Δg and Δf^γ . In preceding studies [14] we have already analyzed jet and heavy flavour production, with the latter turning out to be less useful at collider energies. Here we reanalyze in detail the whole range of conceivable photoproduction processes, covering this time also single-inclusive charged hadron, prompt photon, and Drell-Yan dimuon production. Our previous results for single-inclusive jet production

are extended towards the largest values of the laboratory rapidity η_{LAB} which should be experimentally accessible. At large η_{LAB} one finds an improved sensitivity to Δf^γ . In the case of dijet production we study an additional, less exclusive, kinematic selection (as compared to our previous analysis). This selection allows jets to be measured at higher transverse energies without loss of statistics, and is also more suited to eventual next-to-leading order (NLO) QCD calculations.

It should be stressed that HERA could play a unique role in the determination of the parton content of polarized photons even if it should succeed in establishing only the very existence of a resolved contribution to polarized photon-proton reactions. Other determinations of the Δf^γ , for instance, via a measurement of the photon's spin-dependent structure function g_1^γ in polarized e^+e^- collisions, are not planned in the near future and in case of future lepton-nucleon fixed-target photoproduction experiments such as COMPASS [15], the resolved component is too small to be extracted experimentally [14].

Our previous results, as well as most of those presented here, are based only on leading order (LO) QCD parton level calculations. Of course, in real jet production processes, initial and final state QCD radiation, as well as non-perturbative effects such as hadronization are also present. These lead to multiparticle final states, and necessitate the use of a jet algorithm to recombine the final-state particles into jets. The details of the final-state and the jet algorithm used can in practice lead to significant differences with respect to the parton level results. In general at HERA for jets of the energies considered here, these effects are larger than the smearing introduced by detector resolutions (see, for example [7]). In order to investigate the impact of such effects on the measurement of asymmetries at a polarized HERA, we use a Monte Carlo simulation, SPHINX [16], which includes the polarized matrix elements for jet photoproduction. Here we limit ourselves to the case of dijet production which is the only process that provides a clean separation of the 'resolved' part of the cross section, as will be discussed later. Nevertheless, we expect similar hadronization effects also for single-inclusive jet or hadron production.

Our contribution is organized as follows: In the next section we collect the necessary ingredients for our calculations. Section 3 is devoted to a discussion of the various conceivable photoproduction processes, namely inclusive jet, inclusive hadron, heavy flavour, prompt photon, and dimuon production. Section 4 contains a more detailed investigation of dijet production including our Monte Carlo studies. Finally, section 5 presents the conclusions.

2 Status of the Polarized Parton Distributions of the Proton and the Photon

Even though all recent analyses of polarized DIS [1-3,17] have been carried out at next-to-leading order (NLO) accuracy, we have to stick to LO calculations throughout this work since the NLO corrections to polarized photoproduction processes are not yet known (except for prompt photon production [18] and the 'direct' part of single-inclusive hadron production [19]). This implies use of LO parton distributions, which have been provided in the studies of [1, 2] where various sets, mainly differing in the x -shape of the polarized gluon distribution, were presented.

To study the physics potential of HERA for pinning down Δg in photoproduction processes we will choose four very different LO sets which represent to a good extent the presently large uncertainty in Δg . One should keep in mind that all these sets provide very good descriptions of the present polarized DIS data. For definiteness we will take the LO 'standard' set of the

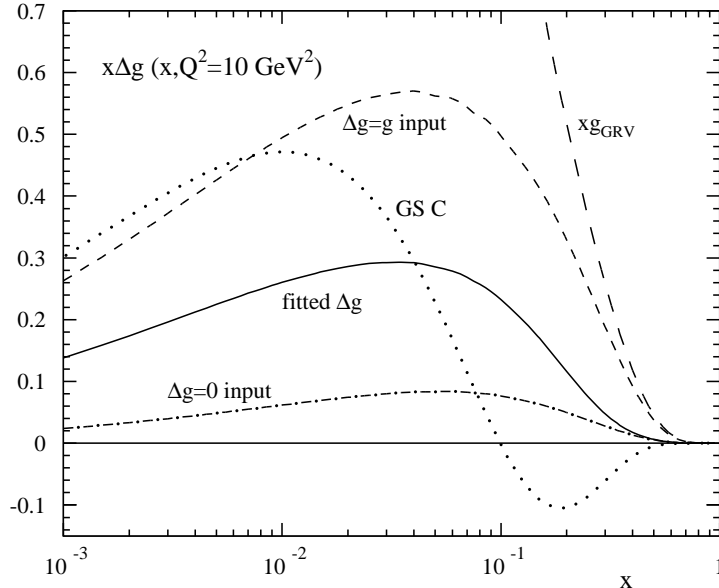


Figure 1: Gluon distributions at $Q^2 = 10 \text{ GeV}^2$ of the four LO sets of polarized parton distributions used. The dotted line refers to set C of [2], whereas the other distributions are taken from [1] as described in the text. Also shown (long-dashed line) is the unpolarized LO gluon distribution of [20].

radiative parton model analysis [1], which corresponds to the best-fit result of that paper¹, along with two other ‘extreme’ sets of [1] which are based on either assuming $\Delta g(x, \mu^2) = g(x, \mu^2)$ or $\Delta g(x, \mu^2) = 0$ at the low input scale μ of [1], where $g(x, \mu^2)$ is the unpolarized LO GRV [20] input gluon distribution. In the following these two sets will be referred to as ‘ $\Delta g = g$ input’ and ‘ $\Delta g = 0$ input’ scenarios, respectively. The gluon of set C of [2], henceforth denoted as ‘GS C’, is qualitatively different as it has a substantial negative polarization at large x . We will therefore also use this set in our calculations. For illustration, we show in fig. 1 the gluon distributions of the four different sets of parton distributions we will use, taking a typical scale $Q^2 = 10 \text{ GeV}^2$. We have also plotted the unpolarized GRV LO gluon distribution in fig. 1, in order to demonstrate that the spin asymmetry for any process sensitive to the gluon is likely to be very small *if* it gets sizeable contributions from the region of small x_{gluon} . This observation has implications for the kinematical cuts we will choose in our phenomenological studies to be presented in the next sections.

In the case of photoproduction the electron just serves as a source of quasi-real photons which are radiated according to the Weizsäcker-Williams spectrum [21]. The photons can then interact either directly or via their partonic structure (‘resolved’ contribution). For a longitudinally polarized electron beam, the resulting photon will be also longitudinally (circularly) polarized and, in the resolved case, the *polarized* parton distributions $\Delta f^\gamma(x, Q^2)$ of the photon enter the calculations. The $\Delta f^\gamma(x_\gamma, Q^2)$ are completely unmeasured so far, so that models for them have to be invoked. To obtain a realistic estimate for the theoretical uncertainties in the polarized photonic parton densities two very different scenarios were considered in [22] assuming ‘maximal’ ($\Delta f^\gamma(x, \mu^2) = f^\gamma(x, \mu^2)$) or ‘minimal’ ($\Delta f^\gamma(x, \mu^2) = 0$) saturation of the fundamental positivity

¹It should be noted that one obtains almost indistinguishable results for all photoproduction cross sections and asymmetries presented in this contribution if one uses the best-fit in the so-called ‘valence’ scenario of [1] instead. These two sets mainly differ in the strange sea-quark content which is of minor importance for our calculations.

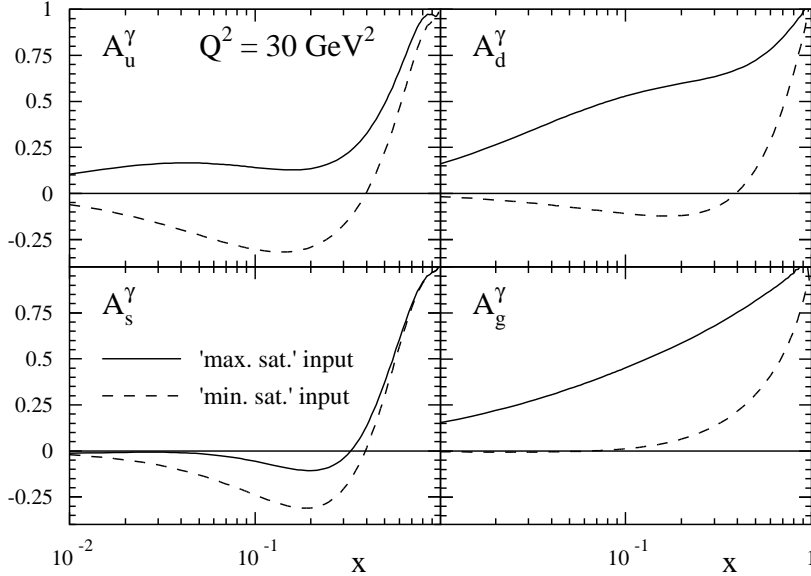


Figure 2: Photonic LO parton asymmetries $A_f^\gamma \equiv \Delta f^\gamma / f^\gamma$ at $Q^2 = 30 \text{ GeV}^2$ for the two scenarios considered in [22] (see text). The unpolarized LO photonic parton distributions were taken from [23].

constraints (similar to the case of nucleons)

$$|\Delta f^\gamma(x, \mu^2)| \leq f^\gamma(x, \mu^2) \quad (1)$$

at the input scale μ for the QCD evolution. Here μ and the unpolarized photon structure functions $f^\gamma(x, \mu^2)$ were adopted from the phenomenologically successful radiative parton model predictions in [23]. The results of these two extreme approaches are presented in fig. 2 in terms of the photonic parton asymmetries $A_f^\gamma \equiv \Delta f^\gamma / f^\gamma$, evolved to $Q^2 = 30 \text{ GeV}^2$ in LO. An ideal aim of measurements in a polarized collider mode of HERA would of course be to determine the Δf^γ and to see which ansatz is more realistic. The sets presented in fig. 2, which we will use in what follows, should in any case be sufficient to study the sensitivity of the various cross sections to the Δf^γ , but also to see how far they influence a determination of Δg .

3 Photoproduction Reactions at Polarized HERA

3.1 General Framework

Let us now turn to some technical preliminaries required for our analyses. First of all, it is useful to define the effective polarized parton densities at a scale M in the longitudinally polarized electron by²

$$\Delta f^e(x_e, M^2) = \int_{x_e}^1 \frac{dy}{y} \Delta P_{\gamma/e}(y) \Delta f^\gamma(x_\gamma = \frac{x_e}{y}, M^2) \quad (2)$$

($f = q, g$), where $\Delta P_{\gamma/e}$ is the polarized Weizsäcker-Williams spectrum for which we will use

$$\Delta P_{\gamma/e}(y) = \frac{\alpha_{em}}{2\pi} \left[\frac{1 - (1-y)^2}{y} \right] \ln \frac{Q_{max}^2(1-y)}{m_e^2 y^2}, \quad (3)$$

²We include here the additional definition $\Delta f^\gamma(x_\gamma, M^2) \equiv \delta(1-x_\gamma)$ for the direct ('unresolved') case.

with the electron mass m_e . For the time being, it seems most sensible to follow as closely as possible the analyses successfully performed in the unpolarized case, which implies to introduce the same kinematical cuts. As in [5, 7, 8, 9, 12] we will use an upper cut³ $Q_{max}^2 = 4 \text{ GeV}^2$, and the y -cuts $0.2 \leq y \leq 0.85$ (for single-jet [5] and heavy flavour [9] production) and $0.2 \leq y \leq 0.8$ (for dijet [7, 8], inclusive hadron [12], prompt photon [13] and Drell-Yan dimuon production) will be imposed.

Furthermore, it should be noted that in what follows a polarized cross section will always be defined as

$$\Delta\sigma \equiv \frac{1}{2} (\sigma(++) - \sigma(+-)) , \quad (4)$$

the signs denoting the helicities of the scattering particles. The corresponding unpolarized cross section σ is obtained by taking the sum instead, and the experimentally relevant cross section asymmetry is $A \equiv \Delta\sigma/\sigma$. Whenever calculating an asymmetry A , we will use the LO GRV parton distributions for the proton [20] and the photon [23] to calculate the unpolarized cross section. For consistency, we will employ the LO expression for the strong coupling α_s with [1, 2, 20, 22, 23] $\Lambda_{QCD}^{(f=4)} = 200 \text{ MeV}$ for four active flavours.

Rapidity distributions will always be presented in terms of the laboratory frame rapidity η_{LAB} which is related to the centre-of-mass η_{cms} via

$$\eta_{cms} = \eta_{LAB} - \frac{1}{2} \ln(E_p/E_e) . \quad (5)$$

As conventional for HERA, η_{LAB} is defined to be positive in the proton forward direction. Studying distributions in η_{LAB} is a particularly suitable way of separating the direct from the resolved contributions in single-inclusive measurements of jets or hadrons: for negative η_{LAB} , the main contributions are expected to come from the region $x_\gamma \rightarrow 1$ and thus mostly from the direct piece at $x_\gamma = 1$. The situation is reversed at positive η_{LAB} .

In the asymmetry plots we will always show the expected statistical errors δA for a measurement at HERA, estimated from

$$\delta A = \frac{1}{P_e P_p \sqrt{\mathcal{L} \sigma \epsilon}} , \quad (6)$$

where P_e, P_p are the beam polarizations, \mathcal{L} is the integrated luminosity and ϵ the detection efficiency for the desired final state. For all our calculations we assume $P_e * P_p = 0.5$ and a conservative value of $\mathcal{L} = 100/\text{pb}$.

3.2 Single-Inclusive Jet Production

For this process we can be rather brief, as all details of the calculation were already described in our previous report [14]. Here we only present updated plots of the cross sections and their asymmetries, extending to larger, but still experimentally accessible, values of η_{LAB} .

Fig. 3 shows our results for the single-inclusive jet cross section and its asymmetry vs. η_{LAB} and integrated over $p_T > 8 \text{ GeV}$ for the four sets of the polarized proton's parton distributions. For figs. 3a,b we have used the 'maximally' saturated set of polarized photonic parton densities, whereas figs. 3c,d correspond to the 'minimally' saturated one. Comparison of figs. 3a,c or 3b,d shows that as expected the direct contribution clearly dominates for $\eta_{LAB} \lesssim -0.5$, where also

³In H1 analyses of HERA photoproduction data [4, 6, 10, 11] the cut $Q_{max}^2 = 0.01 \text{ GeV}^2$ is used along with slightly different y -cuts as compared to the corresponding ZEUS measurements [5, 7, 8, 9, 12], which leads to smaller rates.

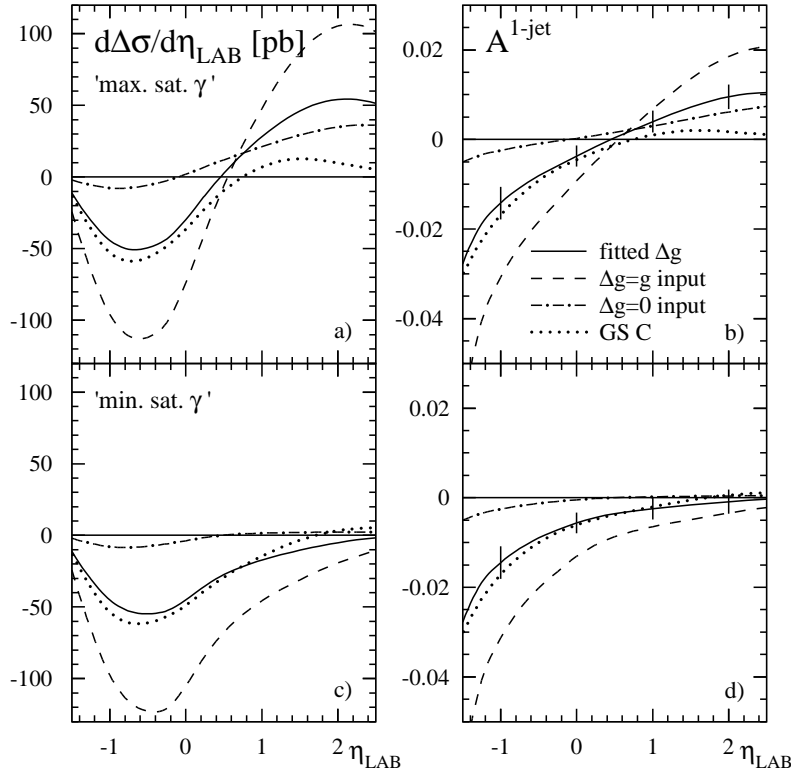


Figure 3: **a:** η_{LAB} dependence of the polarized single-jet inclusive photoproduction cross section in ep -collisions at HERA, integrated over $p_T > 8$ GeV. The renormalization/factorization scale was chosen to be $M = p_T$. The resolved contribution to the cross section has been calculated with the ‘maximally’ saturated set of polarized photonic parton distributions. **b:** Asymmetry corresponding to **a**. The expected statistical errors have been calculated according to (6) and as described in the text. **c,d:** Same as **a,b**, but for the ‘minimally’ saturated set of polarized photonic parton distributions.

differences between the polarized gluon distributions of the proton show up clearly. Furthermore, the cross sections are generally large in this region with asymmetries of a few per cent. At positive η_{LAB} , in particular in the region $\eta_{LAB} \gtrsim 2$ now included in the plot, we find that the cross section is dominated by the resolved contribution. Here it is sensitive to the parton content of both the polarized proton *and* the photon, which means that one can only learn something about the polarized photon structure functions if the polarized parton distributions of the proton are already known to some accuracy, e.g., from an analysis of the region of negative rapidities. We note that the dominant contributions to the resolved part at large η_{LAB} are driven by the polarized photonic *gluon* distribution Δg^γ .

We have included in the asymmetry plots in figs. 3b,d the expected statistical errors δA at HERA estimated from eq. (6) for $\epsilon = 1$. From the results it appears that a measurement of the proton’s Δg should be possible from single-jet events at negative rapidities where the contamination from the resolved contribution is minimal.

3.3 Single-Inclusive Charged Hadron Production

From our results for one-jet production in fig. 3 it seems worthwhile to consider also single-inclusive production of charged hadrons. At first glance, this process appears less interesting

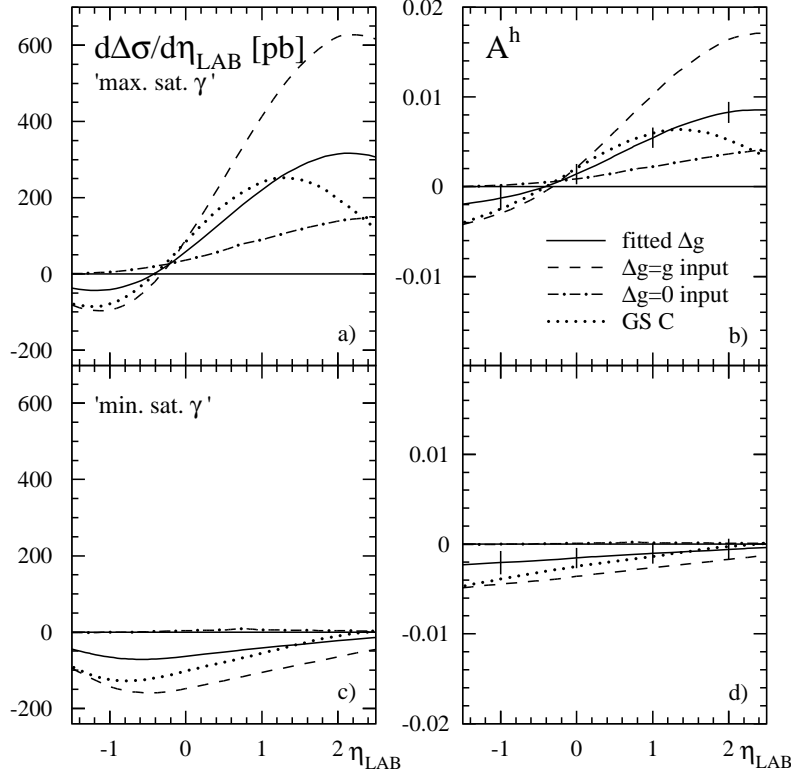


Figure 4: **a:** η_{LAB} dependence of the polarized single-inclusive hadron photoproduction cross section in ep -collisions at HERA, integrated over $p_T > 2$ GeV. The error bars have been calculated assuming an efficiency $\epsilon = 0.8$ for the hadron detection. All other parameters were chosen as in fig. 3.

than jet production, as the cross section for producing a definite hadron at a given p_T will always be smaller than the one for a jet. On the other hand, in case of inclusive hadrons one can obviously go experimentally to p_T much smaller than the $p_T^{min} = 8$ GeV employed in our single jet study. Moreover, in the unpolarized case single-inclusive hadron production was successfully studied experimentally at HERA prior to jets [11, 12].

The generic LO cross section formula for the photoproduction of a single hadron H with transverse momentum p_T and cms-rapidity η in polarized ep collisions reads:

$$\frac{d^2\Delta\sigma^H}{dp_T d\eta} = \sum_{f^e, f^p, c} \Delta f^e(x_e, M^2) \otimes \Delta f^p(x_p, M^2) \otimes \frac{d^2\Delta\hat{\sigma}^{f_e f_p \rightarrow cd}}{dp_T d\eta} \otimes D_c^H(z, M^2), \quad (7)$$

where \otimes denotes a convolution and the sum is running over all appropriate $2 \rightarrow 2$ subprocesses for the direct ($\gamma b \rightarrow cd$, $\Delta f^e(x_e, M^2) \equiv \Delta P_{\gamma/e}(x_e)$) and resolved ($ab \rightarrow cd$) cases. These subprocesses are the same as the ones for jet production. In (7), $\hat{s} \equiv x_e x_p s$ and M is the factorization/renormalization scale for which we will use $M = p_T$ as for our jet calculations. The Δf^p stand for the polarized parton distributions of the proton, and the D_c^H are the unpolarized fragmentation functions for $c \rightarrow H$. For the latter we will use the LO functions of [24] which yield a good description of the unpolarized HERA inclusive hadron data [11, 12]. Needless to say that we obtain the corresponding unpolarized LO jet cross section $d^2\sigma^H/dp_T d\eta$ by using LO unpolarized parton distributions and subprocess cross sections in (7).

Figs. 4a,b show our results for the sum of charged pions and kaons after integration over $p_T > 2$ GeV, where all other parameters were chosen exactly as for figs. 3a,b. One can see

that the spin asymmetries behave rather similarly in shape as the corresponding results in figs. 3a,b, but are somewhat smaller in magnitude mainly due to the smaller x values probed here for $p_T^{\min} = 2$ GeV compared to the single jet case where $p_T^{\min} = 8$ GeV (see also fig. 1). Nevertheless, the expected statistical errors, calculated for the realistic choice of $\epsilon = 0.8$ in eq. (6) and displayed in fig. 4b,d, demonstrate that single-inclusive hadron photoproduction is also a very promising candidate.

We finally mention that apart from charged-hadron production we have also studied the photoproduction of Λ baryons. This is another particularly interesting topic, as it turns out to be possible experimentally to determine the polarization of the produced Λ 's from their parity-violating decays to $p\pi$. This implies that a measurement of the spin asymmetry in this case could allow statements concerning the *spin-dependent* fragmentation functions of the Λ , hereby possibly providing some complementary new insight into 'spin-physics'. Encouraging theoretical predictions for photoproduction of Λ 's are also presented in these proceedings [26].

3.4 Other Processes: Heavy Flavours, Prompt Photons, and Drell-Yan dimuon production

Heavy flavour (charm) production was already considered in our previous report [14], where we found expected statistical errors roughly of the size of the spin asymmetry itself. This process, albeit being very sensitive to Δg thanks to the dominance of the photon-gluon-fusion subprocess $\gamma g \rightarrow c\bar{c}$, appears therefore less favourable than the ones considered in the previous subsections. It is expected to be more useful for fixed-target experiments, where measurements of Δg in open-charm production are planned [15].

Prompt photon production at HERA is currently under investigation in the unpolarized case [13]. Here important contributions at LO result, for instance, from the subprocess $qg \rightarrow \gamma q$, with the initial quark coming from the resolved photon and the gluon from the proton, or vice versa. This process, which is therefore sensitive to Δg in the polarized case, has to compete with $q\bar{q} \rightarrow \gamma g$ annihilation and with the Compton process $\gamma q \rightarrow \gamma q$ from the direct (unresolved) photon. We found that the main problem of prompt photon production is the smallness of the unpolarized cross section (with respect to, say, the single-inclusive hadron cross section), which results in large expected statistical errors, $\delta A^\gamma > A^\gamma$. The experimental study of prompt photon production at a polarized HERA thus appears to be impossible.

Finally, we have also examined photoproduction of Drell-Yan dimuon pairs. This process is of potential interest due to the fact that the relevant LO subprocess is simply $q\bar{q} \rightarrow \mu^+\mu^-$, which means for the case of photoproduction that only the resolved contribution is present at LO. The experimental finding of a nonvanishing asymmetry would therefore be evidence for the existence of polarized (anti)quarks in a polarized real photon. Unfortunately, again the expected statistical errors turn out to be way larger than the asymmetry itself due to the smallness of the unpolarized cross section.

4 Dijet Production

In the case of unpolarized photoproduction of dijets at HERA, an experimental criterion for a distinction between direct and resolved contributions has been introduced [27, 7, 8]. In our previous analysis [14], we have adopted this criterion for the polarized case to see whether it would enable a further access to Δg and/or the polarized photon structure functions. Very encouraging results were obtained. However, the results presented in [14] were based on LO

QCD parton level calculations. One implication of this is that, although the kinematic cuts applied to jets in [14] reflect the cuts which have been used in experimental analyses, the ‘jets’ to which they are applied consist of single quarks or gluons. In a real event, higher order effects such as QCD radiation (in the initial and final state) and non-perturbative effects such as hadronization are also present. These lead to multiparticle final states, and necessitate the use of a jet algorithm to recombine the final state particles into jets. The jet kinematics should then reflect the kinematics of the initiating parton. However, the details of the final state and the jet algorithm used can in practice lead to significant differences with respect to the parton level predictions. In general, at HERA these effects are larger than smearing introduced by detector resolutions (see, e.g., [7]).

In this section, we will therefore present a more sophisticated analysis of dijet production that includes these additional effects, as modelled in the Monte Carlo simulation mentioned in the introduction. Among all our results, the ones presented in this section are therefore the ‘most realistic’ ones. We expect the typical size of the effects from hadronization and QCD radiation found here to be representative for all other photoproduction processes considered in this work.

4.1 Separating Direct and Resolved Contributions

To begin with, let us briefly recall the underlying idea for the separation of direct and resolved contributions [27, 7, 8]. The generic expression for the polarized cross section for the photoproduction of two jets with laboratory system rapidities η_1, η_2 is to LO

$$\frac{d^3\Delta\sigma}{dp_T d\eta_1 d\eta_2} = 2p_T \sum_{f^e, f^p} x_e \Delta f^e(x_e, M^2) x_p \Delta f^p(x_p, M^2) \frac{d\Delta\hat{\sigma}}{d\hat{t}}, \quad (8)$$

where p_T is the transverse momentum of one of the two jets (which balance each other in LO) and

$$x_e \equiv \frac{p_T}{2E_e} (e^{-\eta_1} + e^{-\eta_2}) \quad , \quad x_p \equiv \frac{p_T}{2E_p} (e^{\eta_1} + e^{\eta_2}) \quad . \quad (9)$$

The important point is that measurement of the jet rapidities allows for fully reconstructing the kinematics of the underlying hard subprocess and thus for determining the variable [7]

$$x_\gamma^{OBS} = \frac{\sum_{jets} p_T^{jet} e^{-\eta^{jet}}}{2yE_e} \quad , \quad (10)$$

which in LO equals $x_\gamma = x_e/y$, with y as before being the fraction of the electron’s energy taken by the photon. Thus it becomes possible to experimentally select events at large x_γ , $x_\gamma^{OBS} > 0.75$ [27, 7, 8], hereby extracting the *direct* contribution to the cross section with a relatively small contamination from resolved processes. Conversely, the events with $x_\gamma^{OBS} \leq 0.75$ will represent the resolved part of the cross section. This procedure should therefore be ideal to extract Δg on the one hand, and to examine the polarized photon structure functions on the other.

4.2 Monte Carlo Simulation

In order to investigate the impact of effects from hadronization on the measurement of spin asymmetries at a polarized HERA, a Monte Carlo simulation, SPHINX [16], has been used. SPHINX is based upon the general purpose library of Monte Carlo routines, PYTHIA [28].

As used in this analysis, the program generates hard scatterings according to the LO QCD matrix element, in addition it includes initial and final state QCD radiation calculated to leading

logarithmic accuracy in Q^2 . The parton shower evolves from the scale of the hard interaction down to 1 GeV^2 . Below this scale, the further evolution is considered to be non-perturbative, and the Lund string model is used to hadronize the (in general many) partons.

The additional feature of SPHINX as compared to PYTHIA is that it includes the polarized matrix elements for jet photoproduction, as well as implementing the various different polarized parton distributions (for the proton and photon) discussed previously. Thus the simulation of asymmetries in realistic final states is possible. However, the polarization information is only used in the hard subprocess. The parton showers and fragmentation stages do not preserve a memory of the polarization.

SPHINX/PYTHIA use p_T for the hard scale of the interaction, which is the relative transverse momentum of the scattered partons. Events were generated down to a minimum p_T of 5 GeV .

As a case study, 50 pb^{-1} of luminosity was generated for direct and resolved photoproduction for four options, using the GS C parton distribution for the proton and the maximally and minimally saturated distributions for the photon (36 million events in total). This leaves a pessimistic (or conservative) estimate of the statistical errors which might eventually be obtained, but is sufficient to show whether or not the migrations between parton and hadron level might preserve observable asymmetries.

Most measurements of jet cross sections at hadron-hadron colliders and in photoproduction at HERA have used some variation of a cone-based jet algorithm. These algorithms maximize the transverse energy inside a cone in $\eta - \phi$ space. They are invariant under boosts along the beam axis, and successfully isolate ‘hard’ physics which in hadron-hadron or photon-hadron interactions is generally at large transverse energies with respect to the beam axis. However, they suffer from various ambiguities in how jet finding is initiated in the first place and in how jets are merged or split, and are in general not infrared safe [29].

In this analysis the cluster algorithm KTCLUS [30, 31] is therefore used. In this algorithm, the quantity

$$d_{i,j} = ((\eta_i - \eta_j)^2 + (\phi_i - \phi_j)^2) \min(E_{T_i}, E_{T_j})^2 \quad (11)$$

is calculated for each pair of objects (where the initial objects are the final state particles), and for each individual object:

$$d_i = E_{T_i}^2. \quad (12)$$

If, of all the numbers $\{d_{i,j}, d_i\}$, $d_{k,l}$ is the smallest, then objects k and l are combined into a single new object. If however d_k is the smallest, then object k is a jet and is removed from the sample. This is repeated until all objects are assigned to jets. The parameters for the jet are calculated as:

$$E_T^{jet} = \sum_i E_{T_i} \quad , \quad \eta^{jet} = \frac{1}{E_T^{jet}} \sum_i E_{T_i} \eta_i \quad , \quad \phi^{jet} = \frac{1}{E_T^{jet}} \sum_i E_{T_i} \phi_i \quad (13)$$

in which the sums run over all particles belonging to the jet. This scheme is also used to determine the parameters of the intermediate objects. In this scheme KTCLUS retains the advantages of cone algorithms, without suffering from their associated problems. This algorithm has now been used in more recent experimental analyses (see, e.g., [8]).

4.3 Results for Dijet Production

We first compare the Monte Carlo results with the predictions presented in our previous study. For this purpose we integrate over the cross section in (8) to obtain $d\Delta\sigma/d\bar{\eta}$, where $\bar{\eta} \equiv (\eta_1 +$

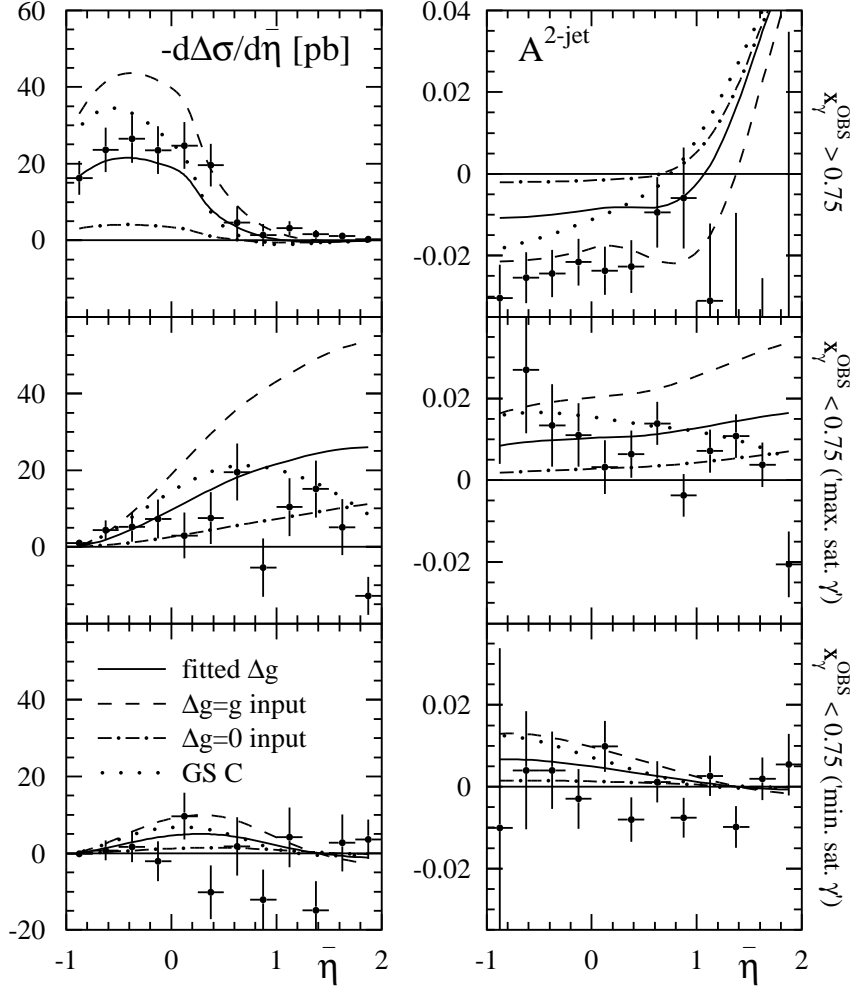


Figure 5: $\bar{\eta}$ -dependence of the ‘direct’ and ‘resolved’ parts of polarized two-jet photoproduction at HERA for the four different sets of polarized parton densities of the proton. The left hand column shows the cross section for $x_\gamma^{OBS} > 0.75$, and for $x_\gamma^{OBS} < 0.75$ with the ‘maximally’ and ‘minimally’ saturated sets of polarized photonic parton densities, reading from top to bottom, respectively. The right hand column shows the corresponding asymmetries. In the top row, the resolved contribution with $x_\gamma^{OBS} > 0.75$ has been included using the ‘maximal’ photon set. Also shown are the Monte Carlo results based on a generated sample of 50/pb using the GS C [2] distributions (see text).

$\eta_2)/2$. Furthermore, we will apply the cuts [7] $|\Delta\eta| \equiv |\eta_1 - \eta_2| \leq 0.5$, $p_T > 6 \text{ GeV}$. The results are shown in fig. 5. The left hand column shows the $d\Delta\sigma/d\bar{\eta}$ distribution for $x_\gamma^{OBS} > 0.75$, and for $x_\gamma^{OBS} < 0.75$ with the ‘maximally’ and ‘minimally’ saturated sets of polarized photonic parton distributions, reading from top to bottom, respectively. The right hand column shows the corresponding asymmetries. The bin widths are chosen to be commensurate with the experimental resolution, rather than being optimized for the size of the statistical sample shown here.

In the high x_γ^{OBS} case ($x_\gamma^{OBS} > 0.75$), the agreement with the parton level predictions is generally good in both the cross section and the asymmetry. The exception is at very forward rapidities ($\eta > 1$) where the parton level cross section is very small and the behaviour of the dijet asymmetry is dominated by the effects of high x_γ^{OBS} resolved contributions and the migration of LO direct jets towards high η due to the presence of the proton remnant (to which they are colour-connected). Nevertheless, overall the prospects for an independent, direct constraint

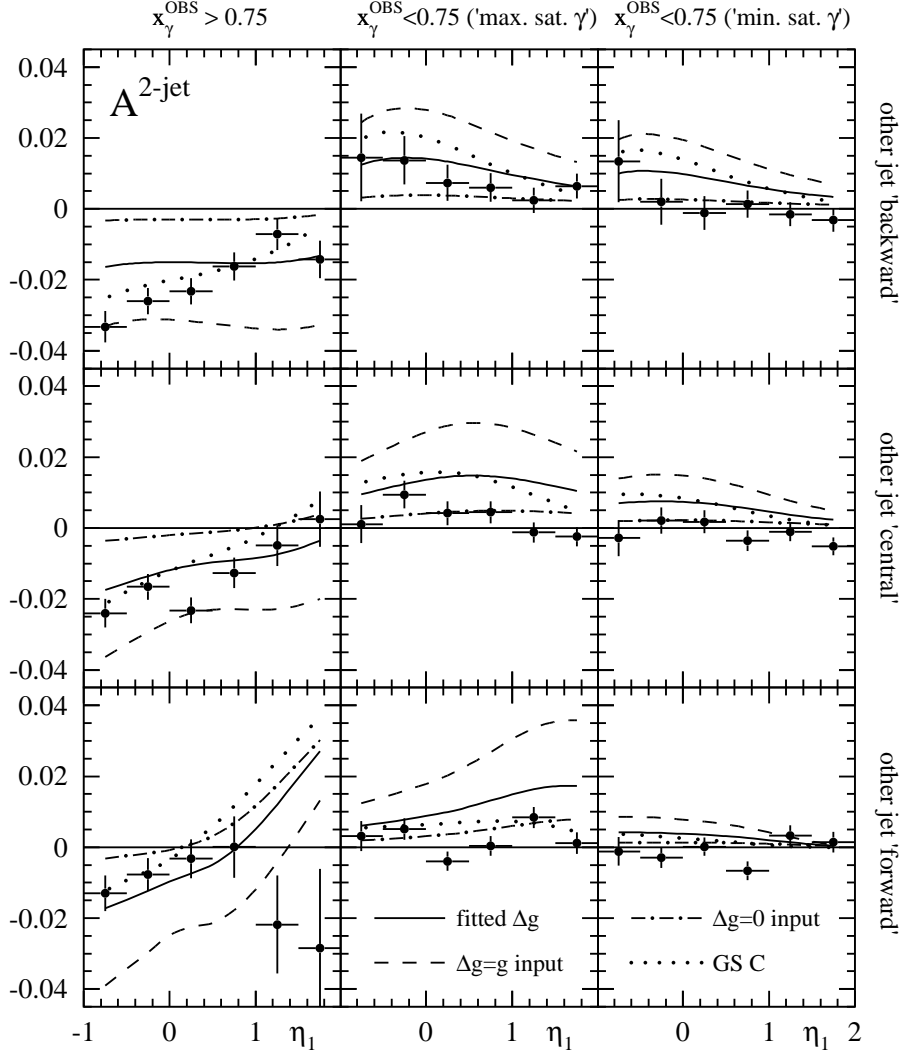


Figure 6: Similar as in fig. 5 but now showing the η_1 -dependence of the polarized two-jet asymmetries at HERA for three different kinematical configurations (see text).

on the polarized parton distributions in the proton by this method appear to be good. In the equally interesting low x_γ^{OBS} case ($x_\gamma^{OBS} < 0.75$), the agreement is not as good, although it is still reasonable. In particular, the minimally saturated case clearly still shows lower asymmetries than the maximally saturated one, and is in fact consistent with zero for this luminosity.

In the unpolarized case, the above cross sections were proposed following arguments based upon LO QCD [27], but have since been calculated to NLO [32]. In the course of these calculations, it was discovered that soft gluon radiation leads to difficulties when the E_T^{jet} threshold is the same for both jets at NLO, and so subsequent measurements have concentrated on cases where a different threshold is applied to each jet. We study here an example of such a cross section. In this case we demand that there must be two jets with $E_T^{jet} > 6$ GeV, as before, but that at least one of them must have $E_T^{jet} > 8$ GeV. The jets are then symmetrized in η . The measured cross sections are then $d\sigma/d\eta_1^{jet}$ for one jet, where the other jet is required to be either ‘backward’ ($-1 < \eta_2^{jet} < 0$), ‘central’ ($0 < \eta_2^{jet} < 2$), or ‘forward’ ($1 < \eta_2^{jet} < 2$). The cross sections are measured for the two regions, $x_\gamma^{OBS} > 0.75$ and $x_\gamma^{OBS} < 0.75$. The $\Delta\eta$ cut is removed. In the LO calculations shown here, which are currently all that is available for such cross sections in the polarized case, both jets of course have the same E_T^{jet} anyway, and so both

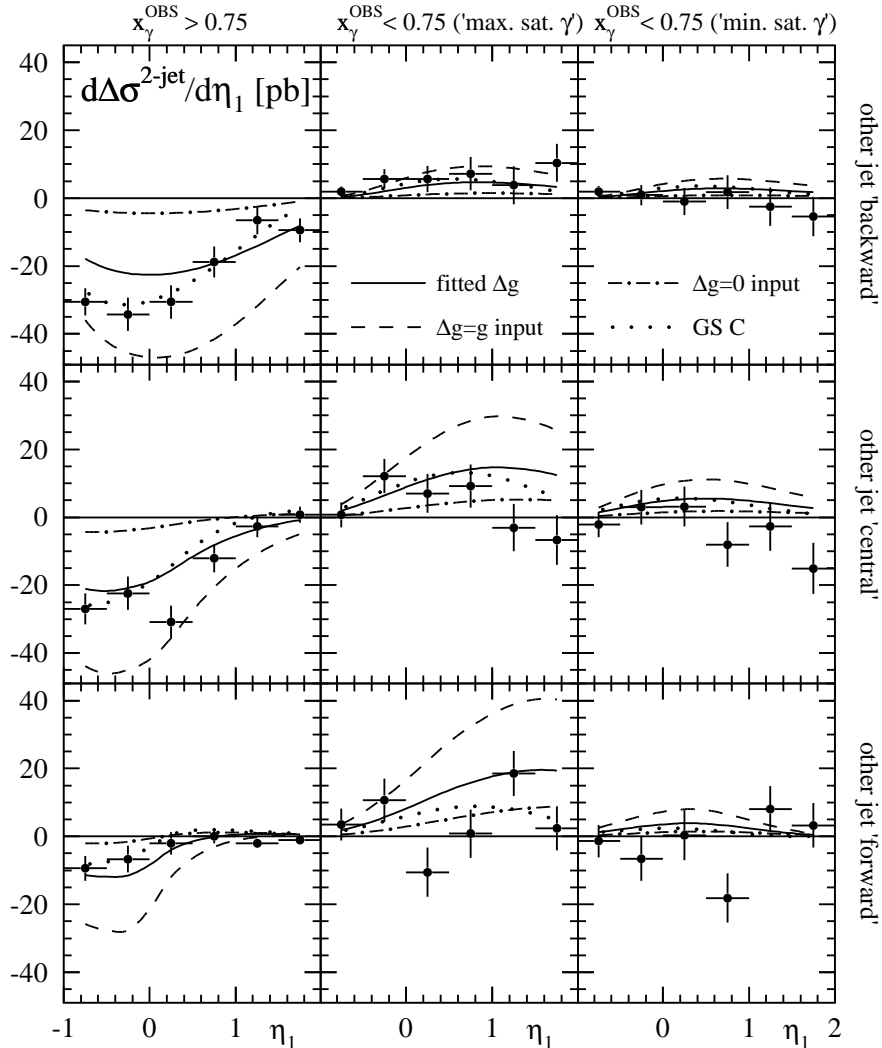


Figure 7: Same as in fig. 6 but now showing the corresponding polarized two-jet cross sections.

have $E_T^{jet} > 8$ GeV. However, in the MC there is smearing due to the additional effects which can lead to jets having different E_T^{jet} .

The results are shown in fig. 6 (asymmetries) and 7 (cross sections). Again in the high x_γ^{OBS} case the agreement is good. In the low x_γ^{OBS} case, the asymmetries are in general lower than in the parton level case, and indeed are consistent with zero for the minimally saturated photonic parton distributions. However, there is still a measurable non-zero asymmetry in the maximally saturated case. The bins widths in these results are dictated by the statistics.

5 Summary and Conclusions

We have analyzed various conceivable photoproduction experiments in the context of a polarized ep -collider mode of HERA. Leading order theory predictions for jet and single-inclusive hadron production show a very encouraging sensitivity to the polarized gluon distribution of the proton and also to the completely unknown parton content of a circularly polarized photon. In particular, it turns out that for these processes the differences between results obtained for different sets of polarized parton distributions are usually clearly larger than the expected statistical errors for a measurement at polarized HERA, even for a rather conservative luminosity of 100/pb. In

contrast to this, the experimental study of photoproduction of heavy flavours, prompt photons and Drell-Yan dimuon pairs at a polarized HERA appears impossible.

In the very promising case of dijet photoproduction which allows for a separation of the ‘direct’ and ‘resolved’ contributions on an experimental basis, we have investigated the impact of parton showering, hadronization and jet finding on the parton level results, which is a crucial ingredient for making contact between theoretical estimates based on LO parton level calculations and the ‘real world’. We have found that although the combined effects of hadronization and QCD radiation can be significant, measurable asymmetries are preserved. Thus the prospects both of obtaining an independent constraint on the polarized parton distributions in the proton, and of observing for the first time a possible asymmetry in those of the photon seem excellent, even with relatively limited integrated luminosity.

Finally, it should be again stressed that HERA could be *the* place to obtain at least some experimental information on the presently completely unmeasured parton distributions of a longitudinally polarized photon in the foreseeable future. Most of the various photoproduction processes studied here appear to be promising and experimentally feasible to achieve this aim even with a conservative luminosity of 100/pb.

References

- [1] M. Glück, E. Reya, M. Stratmann, and W. Vogelsang, *Phys. Rev.* **D53** (1996) 4775.
- [2] T. Gehrmann and W.J. Stirling, *Phys. Rev.* **D53** (1996) 6100.
- [3] D. de Florian, talk presented at the workshop ‘Deep Inelastic Scattering off Polarized Targets: Theory Meets Experiment’, Zeuthen, Germany, 1997, to appear in the proceedings; M. Stratmann, *ibid.*
- [4] I. Abt et al., H1 collab., *Phys. Lett.* **B314** (1993) 436; C. Adloff et al., H1 collab., DESY 97-179, hep-ex/9709017.
- [5] M. Derrick et al., ZEUS collab., *Phys. Lett.* **B342** (1995) 417.
- [6] T. Ahmed et al., H1 collab., *Nucl. Phys.* **B445** (1995) 195; C. Adloff et al., H1 collab., DESY 97-164, hep-ex/9709004.
- [7] M. Derrick et al., ZEUS collab., *Phys. Lett.* **B322** (1994) 287; **B348** (1995) 665.
- [8] J. Breitweg et al, ZEUS collab., DESY 97-196, hep-ex/9710018.
- [9] M. Derrick et al., ZEUS collab., *Phys. Lett.* **B349** (1995) 225; **B401** (1997) 192.
- [10] S. Aid et al., H1 collab., *Nucl. Phys.* **B472** (1996) 32.
- [11] I. Abt et al., H1 collab., *Phys. Lett.* **B328** (1994) 176.
- [12] M. Derrick et al., ZEUS collab., *Z. Phys.* **C67** (1995) 227.
- [13] S. Aid et al., H1 collab., paper submitted to the ‘International Europhysics Conference on High Energy Physics’, 1997, Jerusalem, Israel; J. Breitweg et al., ZEUS collab., DESY 97-146, hep-ex/9708038.

- [14] M. Stratmann and W. Vogelsang, *Z. Phys.* **C74** (1997) 641; Proc. of the 1995/96 workshop on ‘Future Physics at HERA’, Hamburg, Germany, eds. G. Ingelman, A. De Roeck, and R. Klanner, p. 815.
- [15] G. Baum et al., COMPASS collab., CERN/SPSLC 96-14.
- [16] S. Güllenstern et al., hep-ph/9612278; O. Martin, M. Maul, and A. Schäfer, hep-ph/9710381; see also, O. Martin, the SPHINX homepage, <http://www.th.physik.uni-frankfurt.de/~martin/sphinx.html>.
- [17] R.D. Ball, S. Forte, and G. Ridolfi, *Phys. Lett.* **B378** (1996) 255; G. Altarelli, R.D. Ball, S. Forte, and G. Ridolfi, *Nucl. Phys.* **B496** (1997) 337.
- [18] L.E. Gordon and W. Vogelsang, *Phys. Rev.* **D48** (1993) 3136; A.P. Contogouris, B. Kamal, Z. Merebashvili, and F.V. Tkachov, *Phys. Lett.* **B304** (1993) 329; *Phys. Rev.* **D48** (1993) 4092; **D54** (1996) 7081 (E).
- [19] D. de Florian and W. Vogelsang, CERN-TH/97-280, in preparation.
- [20] M. Glück, E. Reya, and A. Vogt, *Z. Phys.* **C67** (1995) 433.
- [21] C.F. von Weizsäcker, *Z. Phys.* **88**, 612 (1934); E.J. Williams, *Phys. Rev.* **45**, 729 (1934).
- [22] M. Glück and W. Vogelsang, *Z. Phys.* **C55** (1992) 353; **C57** (1993) 309; M. Glück, M. Stratmann, and W. Vogelsang, *Phys. Lett.* **B337** (1994) 373.
- [23] M. Glück, E. Reya, and A. Vogt, *Phys. Rev.* **D46** (1992) 1973.
- [24] J. Binnewies, B.A. Kniehl, and G. Kramer, *Phys. Rev.* **D52** (1995) 4947.
- [25] P. Aurenche, A. Douiri, R. Baier, M. Fontannaz, and D. Schiff, *Phys. Lett.* **135B** (1984) 164; *Nucl. Phys.* **B286** (1987) 553; L.E. Gordon, *Phys. Rev.* **D50** (1994) 6753; F. Aversa, P. Chiappetta, M. Greco, and J.Ph. Guillet, *Phys. Lett.* **B210** (1988) 225; **B211** (1988) 465; *Nucl. Phys.* **B327** (1989) 105.
- [26] D. de Florian, M. Stratmann, and W. Vogelsang, hep-ph/9710410, these proceedings.
- [27] J.R. Forshaw and R.G. Roberts, *Phys. Lett.* **B319**, (1993) 539.
- [28] T. Sjöstrand, *Comp. Phys. Comm.* **82** (1994) 74.
- [29] W.T. Giele and W.B. Kilgore, *Phys. Rev.* **D55** (1997) 7183; W.B. Kilgore, talk presented at the ‘32nd Rencontres de Moriond: QCD and High-Energy Hadronic Interactions’, 1997, Les Arcs, France, hep-ph/9705384; M.H. Seymour, hep-ph/9707338.
- [30] S. Catani, Yu.L. Dokshitzer, M.H. Seymour, and B.R. Webber, *Nucl. Phys.* **B406** (1993) 187.
- [31] S.D. Ellis and D.E. Soper, *Phys. Rev.* **D48** (1993) 3160.
- [32] M. Klasen and G. Kramer, *Z. Phys.* **C76** (1997) 67; B.W. Harris and J.F. Owens, *Phys. Rev.* **D56** (1997) 4007.